

# FEEDBACK EFFECTS OF FIRST SUPERNOVAE ON THE NEIGHBORING DARK MATTER HALOS

MASARU SAKUMA

Center for Computational Sciences, University of Tsukuba, Tsukuba, Japan

HAJIME SUSA

Department of Physics, Konan University, Kobe, Japan

*Draft version November 3, 2018*

## ABSTRACT

The first-generation stars in the  $\Lambda$ CDM universe are considered to have formed in dark halos with total masses in the range  $\sim 10^5 - 10^7 M_\odot$  at  $z \sim 20 - 50$ . These stars expected to be very massive and in some cases they end their lives as the first supernovae (SNe). We explore the problem of whether star formation in low mass dark halos ( $\leq 10^7 M_\odot$ ) was triggered or suppressed by the SN feedback from neighboring star-forming halos. We take into consideration mainly two effects by the SN shock: one is the evacuation of gas components from the halos and the other is the promotion of  $H_2$  formation because of the enhanced ionization degree by shock heating. Combining above effects, we find that the star formation activities in the neighboring dark matter halos ( $M \leq 10^7 M_\odot$ ) are basically suppressed in case they are located close to the SN center, because of the gas evacuation effect. The critical distance within which the gas is blown away falls within the range  $\sim 0.3 - 1.5$  kpc depending on the SN energy and the halo mass. In addition, we find there is very little window in the parameter space where star formation activities in dark halos are induced or promoted by neighboring SN.

*Subject headings:* cosmology: theory — hydrodynamics — stars: supernovae: general — ISM: supernova remnants

## 1. INTRODUCTION

Star formation in the early universe has played a critical role in subsequent evolution of the universe. First-generation stars may have substantially contributed to the cosmic reionization and metal pollution of the universe by their radiative/kinetic feedback effects. These events are important for the formation and evolution of protogalaxies. The studies of the initial collapse of primordial pre-galactic objects in the  $\Lambda$ CDM universe have been done in both analytical (Nishi & Susa 1999; Tegmark et al. 1997) and numerical method (Abel et al. 1998; Fuller & Couchman 2000; Yoshida et al. 2003). These objects are formed with masses of the order of  $\sim 10^5 - 10^7 M_\odot$  at redshifts  $z \sim 20 - 50$ . Theoretical studies suggested that in these low-mass halos,  $H_2$  molecules are formed up to the level of  $\sim 10^{-4}$ , because the virial temperature and the central density of these halos are high enough to activate  $H_2$  formation (Nishi & Susa 1999) so that the cooling time becomes short enough. This small fraction of  $H_2$  is sufficient to cool the gas, which leads to the formation of first-generation stars in these halos.

Early studies on the formation of primordial stars have been done in almost one-zone approximation (Carlberg 1981; Hutchins 1976; Matsuda et al. 1965; Palla et al. 1983; Stahler et al. 1986a,b; Susa et al. 1996). On the other hand, after 1990s, there have been a number of numerical studies of the formation of primordial stars (Abel et al. 2000, 2002; Bromm et al. 1999, 2002; Gao et al. 2005; Nakamura & Umemura 1999; Omukai & Nishi 1998; Omukai & Palla 2001; Omukai & Palls 2003; O'shea & Norman 2007;

Yoshida et al. 2006). These studies consistently suggested that first-generation stars are very massive ( $\sim 30 - 500 M_\odot$ ). Because of their extreme mass scale, first-generation stars emit copious amount of ionizing radiation, as well as a strong flux of  $H_2$ -dissociating Lyman-Werner (LW) band radiation. Therefore, the radiation from the first stars dramatically influences their surroundings, heating and ionizing the gas within a few kiloparsecs around the progenitor star.

If the primeval star is very massive ( $\gtrsim 100 M_\odot$ ), the ionization front from the star will break out of parent halos up to  $10^7 M_\odot$  in mass. Half of the baryons in the halo will be swept up into a dense shell that grows to the virial radius of the halo ( $\sim 100$  pc) by the end of the life of the star. Therefore, the gas density within the shell radius will drastically decrease to low uniform densities of  $0.1 - 1 \text{ cm}^{-3}$  prior to the supernova (SN) explosion (Abel et al. 2007; Alvarez et al. 2006; Kitayama et al. 2004; Whalen, Abel & Norman 2004; Wise & Abel 2007).

The dark halos are also affected by the radiation from the first star in the neighboring halos. The local radiative feedback effect is sensitive to the distance from the source star, as well as the mass and the evolutionary stage of the target halo. The ionizing radiation from the star totally or partially photoevaporates them before the SN blast ever reaches them (Ahn & Shapiro 2007; Mesinger et al. 2006; O'shea et al. 2005; Susa & Umemura 2006; Whalen et al. 2008a). Therefore, these halos will be less massive or be gone altogether by the time the SN shock strikes them. It is also should be noted that the LW band radiation from the source star photodissociates  $H_2$  molecules in these halos in case the halos are located close enough to the source (Glover & Brand 2001; Susa 2007).

Some of massive primordial stars end their lives as energetic SNe. Heger & Woosley (2002) suggested that the progenitor star of  $10 - 40M_{\odot}$  dies in Type II SN blasts while those of  $140 - 260M_{\odot}$  dies in pair instability SN. On the other hand, it is important to note that some POP III stars lying in between the ranges indicated above may also explode as hypernovae (Tominaga, Umeda & Nomoto 2007). The studies of first SN explosions have been performed in both SPH (Bromm, Yoshida & Hernquist 2003; Greif et al. 2007) and grid codes (Kitayama & Yoshida 2005; Whalen et al. 2008b). In less massive halos ( $M \lesssim 10^7M_{\odot}$ ), the ejecta first expands into a nearly uniform rarefied ionized medium, then interacts violently with the dense shell swept up in the progenitor H II region. Part of the energy of the blast wave is reflected into the center as a reverse shock and the rest pushes the shell forward (Kitayama & Yoshida 2005; Whalen et al. 2008b). In massive parent halos ( $\gtrsim 10^7M_{\odot}$ ), however, the SN remnant (SNR) will only expand 20 – 40 pc into the halo and then recollapse (Whalen et al. 2008b), never reaching any nearby halos because the *I*-front does not break out these parent halos prior to the SN explosion.

The shock wave from an SN that break away from the host halo impact and go through the neighboring halos those survived photoevaporation process. The shock wave may blow off the gas component; however, it also promote the formation of  $H_2$  and HD molecules in the gas because of the enhanced electron abundance by the shock heating (Ferrara 1998; Johnson & Bromm 2006; Kang & Shapiro 1992; Nishi & Susa 1999; Oh & Haiman 2002; Shapiro & Kang 1987; Susa et al. 1998; Uehara & Inutsuka 2000). We also note that the relic H II region including the photoevaporated halos recombines out of equilibrium, which is basically same physical condition of the postshock enhancement of  $H_2$ /HD formation. The SN shock can sweep up this  $H_2$ /HD and carry it into the nearby halo. Therefore, these molecules in the fossil H II region are important for the formation of secondary stars as well as those would be formed in the SN shock by collisional ionization.

Star formation could be triggered by SNRs in several ways. Primordial SNRs may sweep up a dense shell of ambient gas or collide with the dense shell swept up by an H II region, either of which becomes contaminated by metals in the ejecta, subsequently comes to be dominated by its self-gravity. As a result, the shell is expected to fragment into smaller filaments/cores where populations of less massive stars are formed (Machida et al. 2005; Mackey et al. 2003; Salvaterra et al. 2004; Whalen et al. 2008b). On the other hand, in rather massive halos ( $\gtrsim 10^7M_{\odot}$ ), the H II region generated by the progenitor star is confined well inside the virial radius and the gas is kept neutral. In this case, first SNRs expand in neutral halos, heavily mix their interiors with heavy elements, and then recollapse without escaping the halo (Whalen et al. 2008b).

The interaction of the first SN with neighboring halos in the early universe has not been investigated in detail so far. Recently, Greif et al. (2007) performed a cosmological simulation of first SN explosion. They found that the shock from the SN can accelerate the star formation process in neighboring rather massive halos in which stars could be formed without feedback effects. They also indi-

cated that if the SN explosion occurs in an H II region, the SNR comes to pressure equilibrium at half of the radius of the relic H II region because of its relatively large temperatures. This limits the reach of the SN explosion to  $\sim 1.5$ kpc (Kitayama et al. 2004; Whalen, Abel & Norman 2004). In addition, Cen & Riquelme (2008) performed numerical simulation of SNRs ram-pressure stripping cosmological halos. They focus on how heavy elements from the remnant are mixed with the halo gas.

However, the number of halos studied by numerical simulations is restricted. More analytical criteria are needed in order to obtain a systematic understanding of first SN feedback effects on neighboring dark matter halos. In this paper, we investigate feedback effects by first SN onto the nearby halos in the early universe, which is potentially important for the total star formation activities in the early universe. We use analytic arguments in order to obtain the universal criteria for feedback effects by first SN on the neighboring dark halos. The outline of this paper is as follows. The initial setup and the description of SNR evolution are given in Section 2. In Section 3 and 4, the SN feedback effects are listed and quantified. Section 5 and 6 are devoted to discussion and summary.

## 2. MODEL

We consider SN explosions in the first collapsed halos ( $\lesssim 10^6M_{\odot}$ ). The gravitational potential of these halos are so shallow that the ionizing radiation from the progenitor first stars can sweep out the gas of the host halos (Abel et al. 2007; Alvarez et al. 2006; Kitayama et al. 2004; Whalen, Abel & Norman 2004; Wise & Abel 2007). As a result, the subsequent SNe can easily break away from the halo because of the decreased gas density by photoionization prior to the explosion (Kitayama & Yoshida 2005; Whalen et al. 2008b). In order to understand the nature of the SN shock expanding into an essentially uniform and ionized intergalactic space, we assume spherical symmetry and initially uniform ambient gas density of averaged cosmological density,  $\rho_0$ . Strictly speaking, this assumption is not valid since the gas density of the halo still slightly higher than  $\rho_0$  even after the feedback of UV radiation. This assumption should have some effects to increase the energy of the SN shock, but we use this for simplicity. The energy loss mechanism from the SNR is dominated by bremsstrahlung for a first few years, then line emission, and then inverse Compton scattering becomes important (Kitayama & Yoshida 2005; Whalen et al. 2008b). We take into account all of the cooling rate stated above as well as  $H_2$  cooling at low temperature. We use the fitting formula for these rates from the compilation by Fukugita & Kawasaki (1994) and Galli & Palla (1998), respectively.

We consider the neighboring dark matter halos with total mass of  $10^5M_{\odot} \leq M_{\text{dh}} \leq 10^7M_{\odot}$ , whose baryonic fraction in mass is assumed to be the cosmic mean value,  $\Omega_b/\Omega_M$ . We have another free parameter in our calculations, which is the distance from the SN center to the target halo. Additionally, we use two typical fixed redshift when the SN explode ( $z_{\text{SN}} = 20$ ) and when the nearby halos virialized ( $z_{\text{vir}} = 30$ ). We tested this issue with three different SN explosion energy  $E_{\text{SN}} = 10^{51}, 10^{52}$ , and  $10^{53}$ erg. Throughout the paper, we work with the

$\Lambda$ CDM universe with  $\Omega_M = 0.3$ ,  $\Omega_\Lambda = 0.7$ ,  $h = 0.7$ , and  $\Omega_b = 0.05$ .

### 2.1. Timescales

We introduce three timescales  $t_s$ ,  $t_{\text{cool}}$ , and  $t_{\text{ff}}$ , that characterize the important physical processes. They represent the sound crossing timescale of the gas component in the neighboring halo, the cooling timescale, and the free-fall timescale, respectively. The sound crossing timescale of the gas component in the neighboring halo is described as

$$t_s(l) \equiv \frac{l}{c_s}, \quad (1)$$

where  $l$  denotes the length that we are interested and  $c_s$  is the sound speed of the gas, respectively. This timescale is also interpreted as the expansion timescale of the shock heated gas if we substitute the size of the shock-heated region for  $l$  and use the sound speed of shocked gas as  $c_s$ .

The cooling timescale is defined as

$$t_{\text{cool}}(T) \equiv \frac{nkT}{(\gamma - 1)\Lambda(T, n, f_{\text{H}_2})}, \quad (2)$$

where  $T$  and  $n$  are the temperature and the number density,  $k$  and  $\gamma$  denote the Boltzmann constant and the ratio of specific heats, respectively.  $f_{\text{H}_2}$  represents the fraction of  $\text{H}_2$ , and  $\Lambda$  ( $\text{erg cm}^{-3} \text{s}^{-1}$ ) denotes the cooling rate of gas. The free-fall timescale is written as

$$t_{\text{ff}} \equiv \left( \frac{3\pi}{32G\rho_{\text{vir}}} \right)^{1/2}. \quad (3)$$

Here,  $G$  is the gravitational constant and  $\rho_{\text{vir}}$  is the virial density given by  $\rho_{\text{vir}} \equiv 18\pi^2\rho_{\text{cr}}$ , where  $\rho_{\text{cr}} \equiv 1.9 \times 10^{-29} h^2 (1 + z_{\text{vir}})^3 \text{ g cm}^{-3}$ .

### 2.2. Evolution of SNR

The time evolution of an SNR in intergalactic medium (IGM) is mainly described by following four stages:

- (1) *The free-expansion stage.* The free-expansion stage lasts until the SN ejecta sweeps up roughly the same amount of mass as their own in the surrounding medium. In this stage, the velocity of the SN ejecta decreases linearly with radius (Truelove & Mckee 1999).
- (2) *Sedov–Taylor adiabatic expansion stage.* The expansion of the shock front is well approximated by the Sedov–Taylor solution.
- (3) *Pressure-driven expansion stage.* After the postshock gas is cooled via the radiative cooling, the SNR depart from an adiabatic expansion. Geometrically thin shell is formed just behind the shock front. The expansion of the shocked shell is driven by the high pressure of the hot cavity.
- (4) *Momentum-driven expansion stage.* In this stage, the shocked shell expands conserving its momentum.

In our calculation, we do not take into consideration the stage (1) because the duration of this stage is very short

and it hardly affects the entire result. We also do not consider the stage (4) in IGM since the shock velocity at this stage is too small to activate  $\text{H}_2$  molecule formation or to evacuate the gas from the halo. We consider the scenario, in which the SNR gradually sweeps up mass and then collides with the neighbor halo. In fact, the remnant first collides violently with the dense shell swept up in the progenitor  $\text{H II}$  region, but we leave this effect for future works, since introducing such effect makes the analysis complicated.

#### 2.2.1. The Sedov–Taylor adiabatic stage in IGM

The expansion of the shock front in the Sedov–Taylor adiabatic stage is described by the self-similar solution (Sedov 1946; Taylor 1950). The radius and the expansion velocity of the shock front is written as

$$R_S = 1.15 \left( \frac{E_{\text{SN}}}{\rho_0} \right)^{1/5} t^{2/5}, \quad (4)$$

$$v_S = \frac{dR_S}{dt} = 0.460 \left( \frac{E_{\text{SN}}}{\rho_0} \right)^{1/5} t^{-3/5}, \quad (5)$$

where  $E_{\text{SN}}$  and  $\rho_0$  represent the SN explosion energy and the ambient density, respectively. The postshock temperature is derived from the Sedov–Taylor solution and the Rankine–Hugoniot relation as follows:

$$\begin{aligned} T_{\text{PS}} &= 0.423 \left( \frac{\mu m_{\text{H}}}{k} \right) \frac{(\gamma - 1)}{(\gamma + 1)^2} \left( \frac{E_{\text{SN}}}{\rho_0} \right)^{2/5} t^{-6/5} \\ &= 2.3 \times 10^5 \text{K} \left( \frac{E_{\text{SN}}}{10^{52} \text{erg}} \right) \left( \frac{R_s}{0.5 \text{kpc}} \right)^{-3}, \end{aligned} \quad (6)$$

where  $m_{\text{H}}$  and  $\mu$  denote the atomic mass unit and the mean molecular weight, respectively. These solutions are based upon the assumption, that the gas is adiabatic, however, the postshock gas forms a dense shell which is cooled by the radiative cooling subsequently. After the cooling timescale of the shell becomes shorter than the expansion timescale of the shell ( $t_{\text{cool}} < R_S/v_S$ ), the SNR move on to the pressure-driven expansion stage.

#### 2.2.2. The pressure-driven expansion stage in IGM

The shock front expands by the high pressure in the hot cavity. We assume that the pressure inside the cavity decreases adiabatically as

$$P_{\text{ca}} = P_1 \left( \frac{R_S}{R_1} \right)^{-3\gamma}, \quad (7)$$

where  $P_{\text{ca}}$  denotes the pressure inside the cavity, and also  $R_1$  and  $P_1$  represent the radius of the shock front and the postshock pressure at the beginning of the pressure-driven expansion stage. Combining this equation with the equation of motion of the shell, we have the shock radius/velocity as follows (Sakashita & Ikeuchi 1996).

$$R_S = 1.22 \left( \frac{E_{\text{SN}}}{\rho_0} R_1^2 \right)^{1/7} t^{2/7}, \quad (8)$$

$$v_S = 0.349 \left( \frac{E_{\text{SN}}}{\rho_0} R_1^2 \right)^{1/7} t^{-5/7}. \quad (9)$$

We also obtain the postshock temperature as follows:

$$T_{\text{PS}} = 0.244 \left( \frac{\mu m_{\text{H}}}{k} \right) \frac{(\gamma - 1)}{(\gamma + 1)^2} \left( \frac{E_{\text{SN}}}{\rho_0} R_1^2 \right)^{2/7} t^{-10/7}$$

$$= 1.7 \times 10^4 \text{K} \left( \frac{E_{\text{SN}}}{10^{52} \text{erg}} \right) \left( \frac{R_s}{1 \text{kpc}} \right)^{-5}. \quad (10)$$

### 2.3. Metal cooling

In the present paper, we do not take into account the cooling rate due to heavy elements. In fact, the shock-heated gas in the nearby halos is expected to be polluted by metals ejected from the SN, although the abundance of heavy elements in the shock-heated gas is hard to evaluate. The ultra high resolution simulations would be indispensable to assess the degree of metal mixing. Aside from such difficulty, we can evaluate the metal abundance assuming complete mixing between the SN ejecta and the surrounding material. Based upon such assumption, the mean metallicity of the swept up mass by the SN shock is  $Z/Z_{\odot} \sim 10^{-2.5}$  (Greif et al. 2007; Salvaterra et al. 2004). In addition, the metallicity of the high- $z$  IGM observed by Ly $\alpha$  absorption systems is at a level of  $Z/Z_{\odot} \sim 10^{-3}$  to  $10^{-2}$  (Songaila 2001). Thus,  $Z/Z_{\odot} \sim 10^{-3}$  to  $10^{-2}$  could be a rough standard to assess the effects of metal cooling. At such low metallicity, the radiative cooling rate is hardly affected above  $10^4 \text{K}$  (Boehringer & Hensler 1989), since it is dominated by H and He cooling. The cooling rate below  $10^4 \text{K}$  is basically proportional to the amount of metals (Benjamin et al. 2001; Dalgarno & McCray 1972; Raymond et al. 1976; Raymond & Smith 1977; Sutherland & Dopita 1993), however, again at such low  $Z$ , the metal cooling rate is comparable to  $\text{H}_2$  cooling, as long as  $10^3 \text{K} \lesssim T \lesssim 10^4 \text{K}$  (Susa & Umemura 2004). Therefore, radiative cooling by heavy elements in these halos do not play central role as long as complete mixing is assumed.

On the other hand, metals in the interior of expanding SNR will mix with the shocked shell it sweeps up because of Rayleigh–Taylor and Kelvin–Helmholtz instabilities. This will enrich the shocked region to much higher metallicities than  $Z/Z_{\odot} \sim 10^{-3.5}$ , radiatively cool the shell much faster than any  $\text{H}_2$  it has formed or swept up, and then fragment clumps. It may be a clump that collides with the neighbor halo, not an intact shell, but this is for future numerical studies to determine.

## 3. EFFECTS OF SUPERNOVA SHOCK ON THE NEIGHBORING DARK HALOS

In this section, we assess the effect of the SN shock onto neighboring dark halos by analytic arguments comparing timescales.

### 3.1. Gas evacuation by shock momentum

In case a neighboring halo is located very close to the center of the SN explosion, the gas in the halo would be evacuated by the shock momentum. As a result, subsequent star formation in the halo should be inhibited. Assuming the momentum conservation after the gas behind the shock cools, we can roughly evaluate the velocity of the gas in the halo after the impact of the shocked shell.

In Figure 1, we represent three cases of gas evacuation by shock momentum. First, we consider the simple

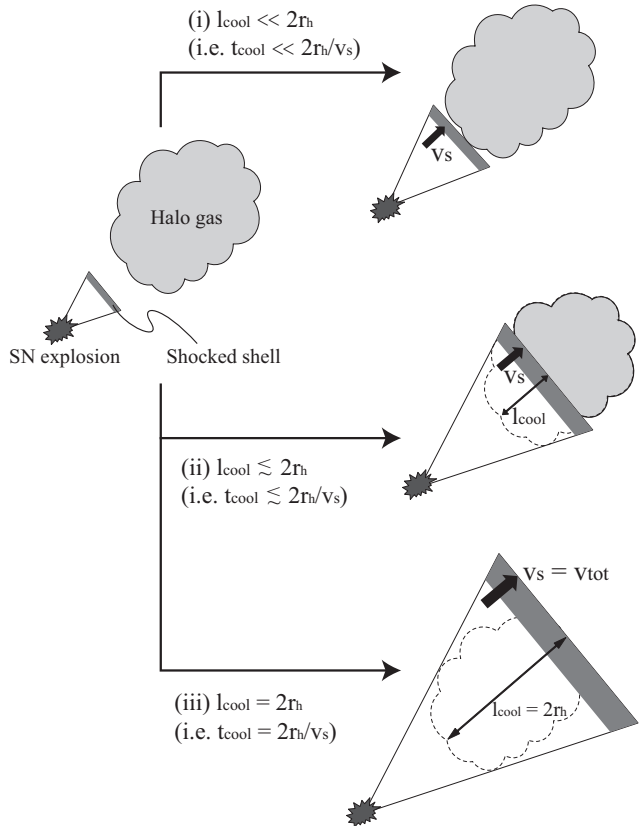


FIG. 1.— Three cases of gas evacuation by shock momentum are represented in this figure. The shock propagates at  $v_s$  before the shocked gas cools by radiative cooling. After that, the shock propagates under the momentum conservation. The intermediate case (case(ii)) indicates that the shock shifts to the momentum-driven expansion phase in the halo.

momentum conserving case (case(i) in Figure 1), where  $l_{\text{cool}} \ll 2r_{\text{h}}$  (i.e.,  $t_{\text{cool}} \ll 2r_{\text{h}}/v_s$ ) is satisfied. Here,  $l_{\text{cool}}$  denotes the distance that the shock sweeps the halo before it enters the momentum conserving phase, i.e.,

$$l_{\text{cool}} \equiv \min(v_s t_{\text{cool}}(T_{\text{PS}}), 2r_{\text{h}}). \quad (11)$$

Here,  $r_{\text{h}}$  is the radius of the dark halo. The equation of the momentum conservation is given as follows:

$$m_S v_S = \left( m_S + \frac{\Omega_b}{\Omega_M} M_{\text{dh}} \right) v_{\text{tot}}, \quad (12)$$

where  $M_{\text{dh}}$  is the mass of the dark halo and  $m_S$  is the mass of the gas shell colliding with the halo, which is given as

$$m_S = \left( M_{\text{POPIII}} + \frac{4}{3} \pi R_S^3 \rho_0 \right) \frac{\pi r_{\text{h}}^2}{4\pi R_S^2}. \quad (13)$$

Here,  $M_{\text{POPIII}}$  is the mass of progenitor POPIII star and we assume that the whole mass of this POPIII star is released as ejecta. We assume  $M_{\text{POPIII}} = 140 M_{\odot}$  in the present calculation.

On the other hand, in case of  $t_{\text{cool}} \lesssim 2r_{\text{h}}/v_s$  (i.e.,  $l_{\text{cool}} \lesssim 2r_{\text{h}}$ , case(ii) in Figure 1), the gas in the halo

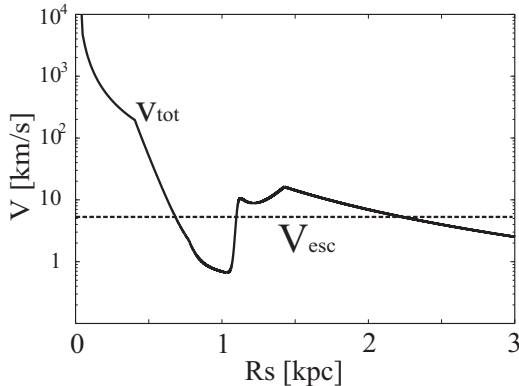


FIG. 2.— Velocity of the shocked gas ( $v_{\text{tot}}$ ) is plotted as a function of the distance from the SN center,  $R_S$ , for  $E_{\text{SN}} = 10^{52}$ erg and  $M_{\text{dh}} = 2 \times 10^5 M_{\odot}$ . The dotted line represents the escape velocity of the halo with  $M_{\text{dh}} = 2 \times 10^5 M_{\odot}$ .

is cooled while the shock propagates in the halo by radiative cooling, and it evolves into the momentum conserving phase. Since the gas pressure of the halo behind the shock front can keep pushing the shock before it cools,  $v_{\text{tot}}$  cannot be estimated by simple momentum conservation equation. It is difficult to assess this effect analytically. Thus, we assume that the shock velocity is not affected by the halo while the radiative cooling is still inefficient even after the shock enters the halo. This assumption could be oversimplification, since even adiabatic shock will slow down to some extent when it enters the dense region. In order to quantify this effect, numerical study would be necessary, which is beyond the scope of present study. Therefore, we have to keep in mind that the shock heating effect is maximally taken into consideration in this model. In this intermediate case (ii) in Figure 1), we assume that the momentum conservation after shocked gas in the halo is cooled:

$$\left(m_S + \frac{l_{\text{cool}}}{2r_h} \frac{\Omega_b}{\Omega_M} M_{\text{dh}}\right) v_S = \left(m_S + \frac{\Omega_b}{\Omega_M} M_{\text{dh}}\right) v_{\text{tot}} \quad (14)$$

In case the shock propagate through the entire halo within the cooling time of the shocked gas, that is the case of  $l_{\text{cool}} = 2r_h$ , the shock velocity in the halo is as large as  $v_S$  during the shock propagation because of the inefficient cooling (case (iii) in Figure 1).

The velocity of the shocked gas shell,  $v_{\text{tot}}$ , is obtained from the equation (14) as follows:

$$v_{\text{tot}} \equiv \frac{m_S + \frac{l_{\text{cool}}}{2r_h} \frac{\Omega_b}{\Omega_M} M_{\text{dh}}}{m_S + \frac{\Omega_b}{\Omega_M} M_{\text{dh}}} v_S. \quad (15)$$

This equation includes all of the three cases. The cases of  $l_{\text{cool}} \ll 2r_h/v_S$  and  $l_{\text{cool}} = 2r_h$  are the limits of efficient/inefficient cooling.

The gas will be still bounded in the halo even after the shock arrival, in case  $v_{\text{tot}}$  is smaller than the escape velocity  $V_{\text{esc}}$  of the halo. On the other hand, if  $v_{\text{tot}} > V_{\text{esc}}$ , the gas is blown away from the halo potential, in which subsequent star formation in the halo is totally quenched. Thus, we regard the condition  $v_{\text{tot}} < V_{\text{esc}}$  as

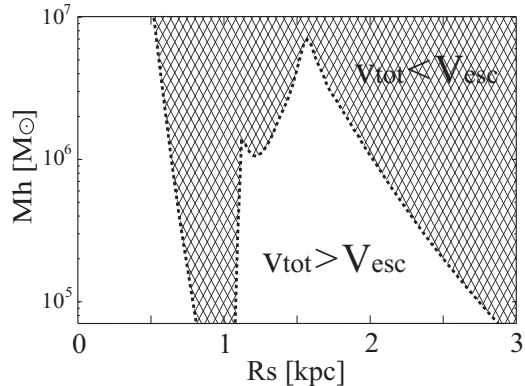


FIG. 3.— Condition of gas evacuation by the SN shock for  $E_{\text{SN}} = 10^{52}$ erg. The horizontal axis shows the distance between the nearby halo and SN center, while the vertical axis denotes the mass of the halo. In the hatched area ( $v_{\text{tot}} < V_{\text{esc}}$ ), the shocked gas is bounded inside the dark halo. The unhatched region labeled as  $v_{\text{tot}} > V_{\text{esc}}$ , the gas will be evacuated by the shock from the SN.

a necessary condition for the triggered star formation in the neighboring dark halos.

In Figure 2,  $v_{\text{tot}}$ , as a function of the distance from the SN center assuming  $M_{\text{dh}} = 2 \times 10^5 M_{\odot}$  and  $E_{\text{SN}} = 10^{52}$ erg. In this case,  $v_{\text{tot}}$  is smaller than  $V_{\text{esc}}$  in the ranges  $0.7 \text{ kpc} \lesssim R_s \lesssim 1.1 \text{ kpc}$  and  $R_s \gtrsim 2.3 \text{ kpc}$ . Therefore, in case the neighboring halo is located at such distance, the gas in the halo is not evacuated by the shock momentum.

Figure 3 shows the gas evacuation from the halos for  $E_{\text{SN}} = 10^{52}$ erg. The vertical axis denotes the mass of the dark matter halos ( $M_{\text{dh}}$ ), whereas the horizontal axis represents the distance from the SN center. In the hatched area denoted as  $v_{\text{tot}} < V_{\text{esc}}$ , the gas in the dark halos are not lost by the shock momentum. It is worth noting that the hatched area around  $R_S = 1 \text{ kpc}$  corresponds to  $T_{\text{PS}} \sim 10^4 \text{ K}$ , where the Ly $\alpha$  cooling dominates the others.

### 3.2. Cooling/collapse of the shocked gas

The halos that satisfies the condition  $v_{\text{tot}} < V_{\text{esc}}$  are able to survive the disruption by the SN shock momentum. As a next step, we consider whether those survived halos can collapse or not. We set the collapse criteria as the condition where the gas temperature is decreased below  $T_{\text{vir}}$ , before the gas cloud expands by the thermal pressure, or bounces by adiabatic compression. In other words, if following conditions

$$t_{\text{cool}}(T) < t_s(l_{\text{cool}}) \quad \text{and} \quad t_{\text{cool}}(T) < t_{\text{ff}}$$

are both satisfied until they cool below the initial virial temperature, we regard that the gas in such halos can collapse to form stars. Here, we consider the sound crossing timescale,  $t_s(l_{\text{cool}}) = l_{\text{cool}}/c_s$ , to be the expansion timescale of the shocked region. In general, the condition  $t_{\text{cool}} < t_{\text{ff}}$  is regarded as the collapse criterion of gravitationally bound system (e.g., Rees & Ostriker 1977). Once this condition is satisfied, the system starts to collapse. The cooling timescale in low-density gas is basically inversely proportional to the density, while the free-fall timescale proportional to the inverse of square root of density. As a result, the ratio  $t_{\text{cool}}/t_{\text{ff}}$  gets smaller

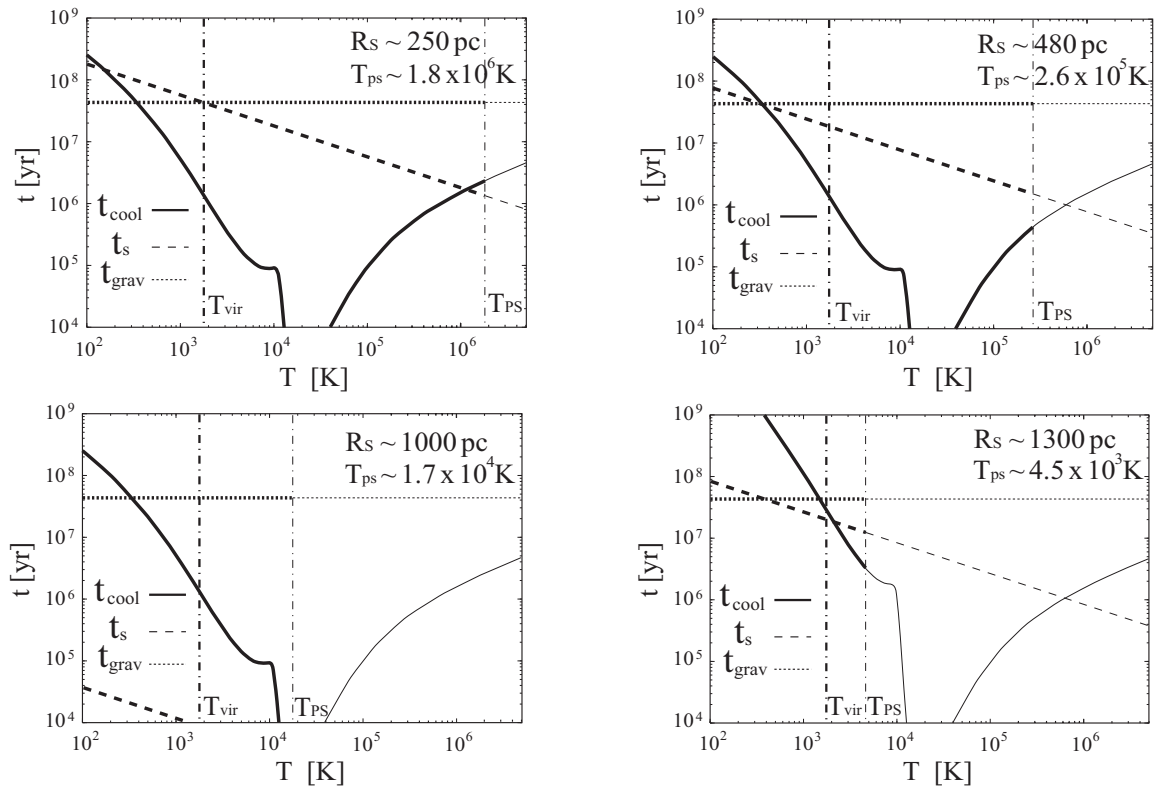


FIG. 4.— Evolution of timescales in the shock-heated gas is shown. Four panels correspond to various distances  $R_S$  (upper-right corner), where the dark halos are located.  $t_{\text{cool}}$ ,  $t_s$ ,  $t_{\text{ff}}$  represent the cooling timescale (solid), the sound crossing timescale of the shock-heated gas (dashed), and the free-fall timescale (dotted), respectively. The thick dot-dashed line indicates the virial temperature of the dark halo in the case of  $M_{\text{vsh}} = 2 \times 10^5 M_{\odot}$ , whereas the thin dot-dashed line shows the postshock temperature  $T_{\text{PS}}$ .

as the collapse proceeds. That's why the condition is regarded as the collapse criterion. In case we consider the primordial star formation, the cooling timescale in most of the final run-away collapse phase is not proportional to the inverse of density, however, the absolute value of the cooling timescale is shorter than the other timescales outside the halo. Thus, the collapse of the cloud continues following the track along which  $t_{\text{cool}} = t_{\text{ff}}$  is satisfied. In addition, we have to consider the adiabatic expansion of the shocked gas, since the sound crossing timescale of the shocked gas could be very short in the present case. Thus, we need to add the inequality  $t_{\text{cool}} < t_s(l_{\text{cool}})$  to the condition of the collapse criteria.

In order to assess this condition, we have to follow the thermal evolution of the shock heated gas in the dark halo. Each of the four panels in Figure 4 shows the evolution of timescales after the shock heating for halos with  $M_{\text{dh}} = 2 \times 10^5 M_{\odot}$  located at  $R_s = 250\text{pc}$ ,  $480\text{pc}$ ,  $1000\text{pc}$ , and  $1300\text{pc}$ . Thermal energy of the SN explosion is assumed as  $E_{\text{SN}} = 10^{52}\text{erg}$ . The horizontal axes denote the temperature of the gas on the way of cooling, whereas the vertical axes show timescales. In order to assess the cooling timescale for  $T \lesssim 10^4\text{K}$ , we have to take into account the  $\text{H}_2$  cooling, which is proportional to  $\text{H}_2$  fraction.  $\text{H}_2$  fraction could be obtained by solving nonequilibrium chemical reaction equations, however, approximate values are already obtained. We use  $f_{\text{H}_2} = 10^{-4}$  in case the postshock temperature,  $T_{\text{PS}}$ , is less than  $10^4\text{K}$  (Nishi & Susa 1999), whereas  $f_{\text{H}_2} =$

$2 \times 10^{-3}$  is employed for  $T_{\text{PS}} > 10^4\text{K}$  (Oh & Haiman 2002; Shapiro & Kang 1987; Susa et al. 1998).

If the halo with  $M_{\text{dh}} = 2 \times 10^5 M_{\odot}$  is located at  $R_s = 250\text{pc}$  (upper-left panel), the shocked temperature is too high for the gas to remain the gas inside the halo potential. In fact, expansion timescale is already shorter than the cooling timescale at  $T = T_{\text{PS}}$ . Thus, the gas in this halo is lost because of the shock heating. On the other hand, in the cases of  $R_s = 480\text{pc}$  (upper-right panel),  $R_s = 1000\text{pc}$  (lower-left panel), and  $R_s = 1300\text{pc}$  (lower-right panel), the gas in the halo can start to cool because  $t_{\text{cool}}(T)$  is smaller than  $t_s(l_{\text{cool}})$  at  $T = T_{\text{PS}}$ . Among these examples,  $t_{\text{cool}}(T)$  is shorter than  $t_{\text{ff}}$  and  $t_s(l_{\text{cool}})$  as long as  $T > T_{\text{vir}}$  is satisfied in the case  $R_s = 480\text{pc}$ . Therefore, the gas can be cooled below  $T_{\text{vir}}$  before it expands, and the cooling phase could be followed by gravitational contraction. In contrast, in the cases of  $R_s = 1000\text{pc}$  and  $R_s = 1300\text{pc}$ , the cooling process becomes inefficient before  $T = T_{\text{vir}}$  is achieved. In the case of  $R_s = 1000\text{pc}$ , the postshock temperature exceeds  $10^4\text{K}$ . Thus,  $f_{\text{H}_2} = 2 \times 10^{-3}$  is achieved even for  $T < 10^4\text{K}$ , whereas  $f_{\text{H}_2} = 10^{-4}$  for  $R_s = 1300\text{pc}$ . Therefore, the cooling condition is not simply determined by the efficiency of  $\text{H}_2$  formation, although it is necessary for the cooling below  $10^4\text{K}$ .

The allowed region for cooling/collapse of the shocked gas is shown in the next section.



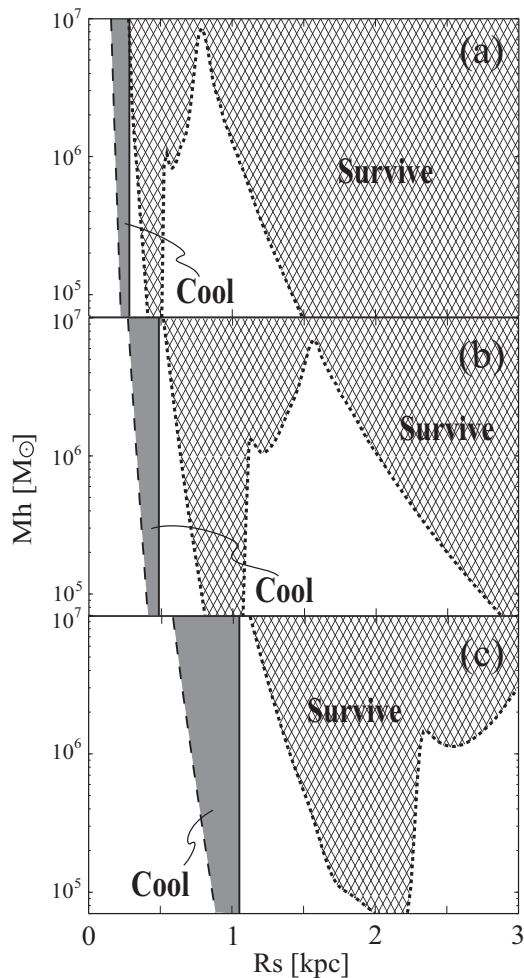


FIG. 5.— Regions in which the shocked gas is cooled and the gas in the dark halos is not evacuated on the  $R_S - M_{\text{dh}}$  plane. Three panels denoted as (a), (b), (c) represent  $E_{\text{SN}} = 10^{51}$ ,  $10^{52}$ , and  $10^{53}$  erg, respectively. In the hatched area labeled as “Survive” ( $v_{\text{tot}} < V_{\text{esc}}$ ), the shocked gas is bounded in the halo potential. On the other hand, in the shaded region denoted as “Cool”, postshock gas cools below  $T_{\text{vir}}$ .

#### 4. POSSIBILITY OF TRIGGERED STAR FORMATION IN THE NEIGHBORING DARK HALOS

Now, we are ready to combine all conditions to find the criteria for positive/negative feedback effects by first SNe on the neighboring dark halos. Three panels in Figure 5 correspond to the results with  $E_{\text{SN}} = 10^{51}$ ,  $10^{52}$ , and  $10^{53}$  erg, respectively. Extremely energetic cases with  $10^{52}$  and  $10^{53}$  erg can be interpreted as the hypernova or the pair-instability SN. The hatched area bounded by dotted curves (labeled as “Survive”) denotes the regions in which  $v_{\text{tot}} < V_{\text{esc}}$  is satisfied. The shaded region denoted as “Cool” represents the condition in which the cooling rate is high enough for the gas in the halo to proceed further gravitational contraction.

First of all, gas components in dark matter halos considered here ( $M \leq 10^7 M_{\odot}$ ) are blown away by the shock momentum if the halos are close enough to the SN center. The critical distance within which the gas is evacuated falls within the range  $\sim 0.3 - 1.5$  kpc depending on the SN energy and mass of the halo. In case we assume normal

core-collapse SN ( $E_{\text{SN}} = 10^{51}$  erg), the critical distance is  $\sim 0.3 - 0.5$  kpc, whereas it is  $\sim 1 - 2$  kpc for pair-instability SN ( $E_{\text{SN}} = 10^{53}$  erg). The mass dependence is not so strong, but basically the low-mass halos are more fragile than the massive halos. In addition, we also note that the boundaries of the ‘Survive’ regions have complicated structures at  $R_S \gtrsim 1$  kpc, reflecting the shape of the cooling function. Recent studies suggested that halos further than  $\sim 1.5$  kpc from the original star will not be reached by the blast. In the present paper, we include distances greater than this in our analysis, but we are doing so only for completeness.

The region where “Survive” and “Cool” are compatible with each other correspond to the case that the shock-heated gas successfully cooled and collapse in the dark halo. However, it is clear that the halos which can survive the evacuation by the SN shock and collapse do not exist. Consequently, the SN feedback has basically negative effects on the star formation in surrounding halos.

#### 5. DISCUSSION

The nearby dark halos come under the influence of the radiation from the SN progenitor star on the satellite halos prior to the explosion. Thus, many low-mass dark halos might be photoevaporated by the UV flux of progenitor star. One-dimensional radiation hydrodynamics simulations are performed by Ahn & Shapiro (2007) on this issue. They found that effects of radiative feedback on the gravitational contraction of the gas in low-mass halos ( $M_{\text{dh}} \lesssim 10^6 M_{\odot}$ ) are very complicated. The feedback effects are qualitatively different depending on the distance from the source star, evolutionary stage of the halo at the onset of radiative feedback, and mass of the halo. Whalen et al. (2008a) also have investigated on this problem by two-dimensional radiation hydrodynamics simulations, for a single halo with mass of  $M_{\text{dh}} = 1.35 \times 10^5 M_{\odot}$ , in which they take into account a detailed evolutionary stage of the halo. They found that most of the gas in this halo is photoevaporated by the SN progenitor star prior to its death at very early evolutionary stages of the halo. On the other hand, they indicated that the  $I$ -front could not reach the core of the halo and this core survived quite well if central densities of the halo rose beyond  $50 \text{ cm}^{-3}$ . Yoshida et al. (2007) also performed three-dimensional radiation hydrodynamics simulations with realistic cosmological density field. They found the H II region of  $100 M_{\odot}$  POPIII star extend to  $\sim 1$  kpc, within which most of low-mass halos are photoevaporated. However, the number of survived halos through UV flux from progenitor star is still under debate, since we only have the results by multidimensional simulations with restricted parameter space (mass of the halo, mass of the progenitor star). In any case, it is worth to investigate the effects of SN shock on the nearby halos with various parameters by analytical calculations.

In our study, we completely ignore mass loss in the neighbor halos due to photoevaporation by the progenitor star. Therefore, it must be noted that our results are taken to be a lower limit on the damage done by the expanding remnant to the halo because the halos the SN blast actually encounters will have less gas. Also the negative feedback effect we have found applies only to the one scenario, in which the SNR increasingly sweeps up mass and then collides with the neighboring halo. It

could be that SN directly form more stars by other means than those they quench in nearby halos in our mechanism.

## 6. CONCLUSION

We have studied the feedback effects by first SNe with  $E_{\text{SN}} = 10^{51}$ ,  $10^{52}$ , and  $10^{53}$  erg on their neighboring dark matter halos. Consequently, the conclusion can be summarized as follows. We find that the star formation activities in the neighboring dark matter halos ( $M \leq 10^7 M_{\odot}$ ) are basically suppressed in case they are located close to the SN center, because of the gas evacuation effect. The critical distance within which the gas is blown away falls within the range  $\sim 0.3 - 1.5$  kpc depending on the SN energy and the halo mass. In case we assume normal core-collapse SN ( $E_{\text{SN}} = 10^{51}$  erg), the critical distance

is  $\sim 0.3 - 0.5$  kpc, whereas it is  $\sim 1 - 1.5$  kpc for pair-instability SN ( $E_{\text{SN}} = 10^{53}$  erg). In addition, we find there is very little window in the parameter space where star formation activities in dark halos are induced or promoted by neighboring SN.

We thank the anonymous referee for critical comments to improve the paper. We also thank T. Kitayama, D. Sato, M. Umemura, & K. Ohsuga for fruitful discussions and useful comments. The analysis has been made with computational facilities at Center for Computational Sciences in University of Tsukuba and Rikkyo University. This work was supported in part by Ministry of Education, Culture, Sports, Science, and Technology (MEXT), Grants-in-Aid, Specially Promoted Research 16002003.

## REFERENCES

- Abel, T., Anninos, P., Norman, M. L., & Zhan, Y. 1998, *ApJ*, 508, 518A
- Abel, T., Bryan, G. L., & Norman, M. L. 2000, *ApJ*, 540, 39
- Abel, T., Bryan, G. L., & Norman, M. L. 2002, *Science*, 295, 93
- Abel, T., Wise, J. H., & Bryan, G. L. 2007, *ApJ*, 659, L87
- Ahn, K., & Shapiro, P. R. 2007, *MNRAS*, 375, 881
- Alvarez, M. A., Bromm, V., & Shapiro, P. R. 2006, *ApJ*, 639, 621
- Benjamin, R. A., Benson, B. A., & Cox, D. p. 2001, *ApJ*, 554, L225
- Boehringer, H., & Hensler, G. 1989, *A&A*, 215, 147
- Bromm, V., Coppi, P. S., & Larson, R. B. 1999, *ApJ*, 527, L5
- Bromm, V., Coppi, P. S., & Larson, R. B. 2002, *ApJ*, 564, 23
- Bromm, V., Yoshida, N., & Hernquist, L. 2003, *ApJ*, 596L, 135B
- Carlberg, R. G. 1981, *MNRAS*, 197, 1021
- Cen, R. & Riquelme, M. A. 2008, *ApJ*, 674, 644C
- Dalgarno, A. & McCray, A. 1972, *ARA&A*, 10, 375
- Ferrara, A. 1998, *ApJ*, 499, L17
- Fukugita, M., & Kawasaki, M. 1994, *MNRAS*, 269, 563
- Fuller, T. M., & Couchman, H. M. P. 2000, *ApJ*, 544, 6
- Galli, D., & Palla, F. 1998, *A&A*, 335, 403
- Gao, L., White, S., Jenkins, A., Frenk, C., & Springel, V. 2005, *MNRAS*, 363, 379
- Greif, T. H., Johnson, J. L., Bromm, V., & Klessen, R. S. 2007, *ApJ*, 670, 1G
- Glover, S & Brand, P. 2001, *MNRAS*, 321, 385
- Heger, A., & Woosley, S. E. 2002, *ApJ*, 567, 532H
- Hutchins, J.B. 1976, *ApJ*, 205, 103
- Johnson, J. L., & Bromm, V. 2006, *MNRAS*, 366, 247
- Kang, H., & Shapiro, P. R. 1992, *ApJ*, 386, 432
- Kitayama, T., Yoshida, N., Susa, H., & Umemura, M. 2004, *ApJ*, 613, 631
- Kitayama, T., & Yoshida, N. 2005, *ApJ*, 630, 675
- Machida, M. N., Tomisaka, K., Nakamura, F., & Fujimoto, M. Y. 2005, *ApJ*, 622, 39
- Mackey, J., Bromm, V., & Hernquist, L. 2003, *ApJ*, 555, 92
- Matsuda, T., Sato, H., & Takeda, T. 1965 *Prog. Theor. Phys.* 42, 219
- Mesinger, A., Bryan, G. L., & Haiman, Z. 2006, *ApJ*, 648, 835M
- Nakamura, F., & Umemura, M. 1999, *ApJ*, 515, 239
- Nishi, R., & Susa, H. 1999, *ApJ*, 523, L103
- Oh, S. P., & Haiman, Z. 2002, *ApJ*, 569, 558
- Omukai, K., & Nishi, R. 1998, *ApJ*, 508, 141
- Omukai, K., & Palla, F. 2001 *ApJ*, 561L, 55O
- Omukai, K., & Palla, F. 2003 *ApJ*, 589, 677O
- O'shea, B. W., Abel, T., Whalen, D., & Norman, M. L. 2005, *ApJ*, 628L, 5O
- O'shea, B. W., & Norman, M. L. 2007, *ApJ*, 654, 66
- Palla, F., Salpeter, E. E., & Stahler, S. W. 1983, *ApJ*, 271, 632
- Raymond, J. C., Cox, D. P., & Smith, B. W. 1976, *ApJ*, 204, 290
- Raymond, J. C., & Smith, B. W. 1977, *ApJS*, 35, 419
- Rees, M. J., & Ostriker, J. P. 1977, *MNRAS*, 179, 541
- Sakashita, S., & Ikeuchi, S. 1996, *Astronomical Hydrodynamics* (Tokyo: Baifukan)
- Salvatera, R., Ferrara, A., & Schneider, R. 2004, *New Astron.*, 10, 113
- Sedov, L. I. 1946, *Prikl. Mat. Mekh.*, 10 (2), 241
- Shapiro, P. R., & Kang, H. 1987, *ApJ*, 318, 32
- Songaila, A. 2001, *ApJ*, 561, L153
- Stahler, S. W., Palla, F., & Salpeter, E. E. 1986a, *ApJ*, 302, 590S
- Stahler, S. W., Palla, F., & Salpeter, E. E. 1986b, *ApJ*, 308, 697S
- Susa, H., Uehara, H., & Nishi, R. 1996, *Prog. Theor. Phys.*, 96, 1073
- Susa, H., Uehara, H., Nishi, R., & Yamada, M. 1998, *Prog. Theor. Phys.*, 100, 63
- Susa, H., & Umemura, M. 2004, *ApJ*, 600, 1
- Susa, H., & Umemura, M. 2006, *ApJ*, 645L, 93S
- Susa, H. 2007, *ApJ*, 659, 908
- Sutherland, R. S., & Dopita, M. A. 1993, *ApJS*, 88, 253
- Taylor, G. I. 1950, *Proc. R. Soc. London A*, 201, 159
- Tegmark, M., Silk, J., Rees, M. J., Blanchard, A., Abel, T., & Palla, F. 1997, *ApJ*, 474, 1
- Tominaga, N., Umeda, H., & Nomoto, K. 2007, *ApJ*, 660, 516T
- Truelove, J. K., & McKee, C. F. 1999, *ApJS*, 120, 299
- Uehara, H., & Inutsuka, S.-i. 2000, *ApJ*, 531, L91
- Whalen, D., Abel, T., & Norman, M. L. 2004, *ApJ*, 610, 14
- Whalen, D., O'shea, B. W., Smidt, J., & Norman, M. L. 2008a, *ApJ*, 679, 925W
- Whalen, D., van, V. B., O'shea, B. W., & Norman, M. L. 2008b, *ApJ*, 682, 49W
- Wise, J. H., & Abel, T. 2007, *ApJ*, 685, 40
- Yoshida, N., Abel, T., Hernquist, L., & Sugiyama, N. 2003, *ApJ*, 592, 645
- Yoshida, N., Omukai, K., Hernquist, L., & Abel, T. 2006, *ApJ*, 652, 6Y
- Yoshida, N., Oh, S. P., Kitayama, T., & Hernquist, L. 2007, *ApJ*, 663, 687